Mars Orbiter Camera observation of linear and curvilinear features in the Hellas basin: Indications for multiple processes of formation

Jens Ormö
Centro de Astrobiología, Instituto Nacional de Técnica Aeroespacial, Madrid, Spain

Goro Komatsu
International Research School of Planetary Sciences, Universita d'Annunzio, Pescara, Italy

Received 13 September 2002; revised 12 March 2003; accepted 8 April 2003; published 21 June 2003.

[1] The high resolution of the Mars Orbiter Camera images reveals many detailed landforms on Mars' surface, which include thin dark or bright linear/curvilinear features. The latter are generally only a few tens of meters wide but can be a couple of kilometers in length. Some of these features have previously been attributed to the action of dust devils. Our study of the linear/curvilinear features in the Hellas basin reveals a variety that can only be explained by the formation from many different processes. In order to evaluate different causes for their formation we created a mapping based on a classification scheme where the linear/curvilinear features were sorted into three groups and compared to terrestrial analogues. Features in group 1 are most frequent, and contain streaks that appear only to affect the ground surface. The best analogue is dust devil tracks. The second, very rare, group appears to penetrate the surface in a way expected of fractures. In the third, likewise rare, group the features have a topographic expression that makes them similar to grooves and/or trenches between narrow ridges. This group is probably formed by multiple processes. Possible terrestrial analogues are found in glacial and periglacial environments (e.g., glacial scouring, fluted moraine, cryoturbation patterns, and iceberg plow marks). The existence of such landforms in the Hellas basin is consistent with previously presented glacial models and has an important implication for the understanding of the past climatic evolution of Mars. *INDEX TERMS:* 6225 Planetology: Solar System Objects: Mars; 6207 Planetology: Solar System Objects: Comparative planetology; 6061 Planetology: Comets and Small Bodies: Remote sensing; 5416 Planetology: Solid Surface Planets: Glaciation; 4540 Oceanography: Physical: Ice mechanics and air/sea/ice exchange processes; *KEYWORDS:* frozen ground, paleoclimatology, glaciation, remote sensing, surface materials and properties, Mars

Citation: Ormö, J., and G. Komatsu, Mars Orbiter Camera observation of linear and curvilinear features in the Hellas basin: Indications for multiple processes of formation, *J. Geophys. Res.*, *108*(E6), 5059, doi:10.1029/2002JE001980, 2003.

1. Introduction

[2] The Mars Orbiter Camera (MOC) on board the Mars Global Surveyor (MGS) has acquired a large number of images of the Martian surface with very high spatial resolutions (1.5–12 m). This has enabled the identification of small-scale surface features, many of which have not been previously described. This study has focused on enigmatic linear and curvilinear features (hereinafter referred to as LCFs) that in general are visible as thin dark, or rarely white lines in satellite images of the Martian surface. Some of the features are in such abundance that they are even visible in Viking images. *Veverka* [1976] described these features as "dark filamentary markings" and suggested a relation to wind activity. He was, however, uncertain if they were erosional or depositional in character. *Grant and Schultz* [1987] described lineations in the Martian northern plains that ranged 2 km to 75 km in length and were less than 1 km wide. The lineations were supposed to originate from tornado-like vortices. Such vortices, caught in action by the Viking Orbiter camera, had been described by *Thomas and Gierasch* [1985]. It was evident that these "dust devils" were a common feature in smooth plains and that they could redistribute large quantities of dust. The generation of tracks by removal of dust by dust devils is presently being studied in laboratory experiments [*Greeley et al.*, 2001; *Balme et al.*, 2002]. The LCFs described in our study, using MOC images, are in general 10–100 m wide and a few hundred to a few kilometers long. LCFs in this size range have been observed on many locations on Mars by other researchers [e.g., *Malin and Edgett*, 2001]. Often the LCFs have been attributed to the effects of dust devils. Active dust devils have been observed on Mars' surface not

0148-0227/03/2002JE001980$09.00

only by Viking orbital imagery, but also in MOC images and by the camera on the Pathfinder lander [e.g., *Malin and Edgett*, 2001; *Metzger et al.*, 1999]. The MOC analyses by *Malin and Edgett* [2001] showed active dust devils creating trails. From this it is evident that many LCFs are indeed dust devil tracks. Support for this conclusion is also provided by multitemporal observations of LCFs that change from image to image. Possible dust devil tracks have recently been identified in terrestrial high-resolution satellite images of the Sahara. These tracks are very similar in appearance to the Martian LCFs [*Rossi*, 2002]. LCFs in the Hellas basin were first recognized and discussed by *Komatsu et al.* [1999] using MOC images. Although the examples were limited, they interpreted some of the LCFs to be glacier scour marks in association with hypothesized ancient glaciation in the basin, an idea originally proposed by *Kargel and Strom* [1992]. In another analysis, *Komatsu et al.* [2000] noted similarities between some LCFs and iceberg scour marks (iceberg plow marks) commonly observed on the seafloor along the Arctic and Antarctic coasts. Iceberg plow marks form when icebergs drift into areas with water depths less than the iceberg keel depth. One image of LCFs [*Ormö et al.*, 2001, Figure 1] suggested that some linear features are indeed trenches, providing further support for the iceberg scour mark hypothesis. However, earlier studies had a number of limitations in their interpretations, primarily because of small spatial and temporal coverage of released MOC images. In our work, we expand earlier studies with more newly released data in order to examine the LCFs' geographical distribution and temporal changes, and to conduct detailed geomorphological analysis of the features.

2. Method

[3] This study is based on remote sensing using MOC images. The aim is to find the origin(s) of various LCFs that occur on the Martian surface. The characterization of their appearance was the first step toward this goal. These results were then compared to similar surface features on Earth.

[4] In the initial stage, ~1700 randomly selected, globally distributed MOC images were analyzed for the occurrence of LCFs. This gave an overview of the variety of LCFs on Mars, and their global and regional distribution. In this survey, it was noticed that LCFs were especially frequent in the Hellas basin. There they also show a great variation in their appearance, which enables comparative studies. Hence the second stage of the study focused on the LCFs in the Hellas basin. We used all images over the interior and close surroundings of the Hellas basin that have been released to date from mission phases dating from September 1997 to August 1999 and September 1999 to February 2000. A total of 108 images contained visible LCFs. In a few cases we used more recent images to investigate the consistency of the occurrence of selected LCFs of interest.

[5] The LCFs in each MOC image were catalogued with respect to variations in width, linearity, spacing, outline (crisscrossed or parallel), terrain, and amount of apparent penetration of the subsurface. Of the 108 images classified in this way, only a few of special interest are listed in Table 1 (due to the limited space). The catalogued LCFs were then classified into groups based on similarities in their appearance. Each individual occurrence of an LCF does not necessarily have the same genesis as the others in the group. Many processes generate similar features. Therefore the different causes of formation of LCFs within each group were identified based on (1) their topographic and regional location, (2) their individual appearance, (3) previously published paleoenvironmental context, and (4) comparisons with published analogues on Mars and Earth.

[6] The location of each image containing LCFs was mapped and color coded based on our group classification. Even corrupt images or images with no visible LCFs were indicated in the map. It was also noted in the map if the LCFs had a preferred direction.

[7] In some cases LCFs from different groups occur in the same image. The color code indicates the most dominant group of LCFs in the image. A separate color code was used when two groups of LCFs were equally common in the image. The mapping gives the regional distribution of different LCFs. The distribution was compared to the topography of the Hellas basin using Mars Orbiter Laser Altimeter data (MOLA).

[8] The temporal variation of the LCFs was analyzed by studying two images of the same area, but from different times of acquisition. The areas selected for this analysis had a very dense population of LCFs.

[9] For reference, we also investigated the influence of resolution and incidence angle on the visibility of the LCFs. It is important to know if these parameters may affect our interpretations. Images from a southern sector of the Hellas basin were selected. Comparisons were made between images classified as "empty" of LCFs and images with clearly visible ("good") LCFs. Corrupt images were not included. A higher image resolution would, theoretically, help in the detection of LCFs because some of them are faint and thin. The incidence angle is the angle between the Sun and a "normal" drawn perpendicular to the planet's surface at the time the image is acquired. A higher incidence angle means that a person on the ground would see the Sun lower toward the horizon. The incidence angle may affect the visibility of surface features. A low incident angle may enhance albedo differences, such as dust devil tracks, whereas a high incident angle could enhance the appearance of topographic features due to shadows in, for example, grooves.

3. Mapping Results and Classification

[10] The first overview of globally distributed MOC images revealed that LCFs occur at all latitudes, at various geological settings, and at different altitudes on Mars. They also show a number of variations in their appearance. Some are clearly the result of eolian processes, especially dust devils, others of tectonism, volcanism or even slope processes [e.g., *Edgett et al.*, 2000; *Albin and King*, 2001]. However, many remain enigmatic, especially in the Hellas basin. In this area, LCFs occur in the majority of the MOC images examined by our study and are often highly dense.

[11] The LCFs in the Hellas basin give a good representation of the diversity of the Martian LCFs. They are, in general, seen as dark lines of a few kilometers length. Some are crossing dunes and other apparently soft materials

Table 1. Criteria for Classifications of All Studied MOC Images in the Hellas Basin That Contained LCFs[a]

	Width		Linearity		Spacing			Outline		Terrain		Apparent Surface Penetration			
MOC Image	Varying	Equal	Curved	Straight or Bent	Detached	Free	Wide	Many Directions	Preferred Direction	Smooth	Rough	Surficial	Penetrative	Grooved	Interpretation
M1002813	x		x		x			x	(x)		x	x			dd
M1201292	x		(x)	x	x			(x)	x		x	x			dd
AB110103		x		x	x				x			x			dd
M0903721	x		x	(x)		x		(x)	x		x	x			fluv
M1200407	x		x			x		x			x		x		fr
M1001828	x		x		x			x			x		x		fr
M0701980		x		x		x			x		x		x		fr
M0701142	(x)	x		x	x			(x)	x		x	?	?		fr + dd
M0906395		x		x	x				x		(x)		x	?	fr
	x			x			x		x		x	x			dd
M0203070		x		x		x			x		x		?	?	gr
M0403935	x			x		x			x	x			?	?	gr
M0202679		x		x	x				x	x				x	gr
M1002592		x		x	x				x		?			x	gr
			(x)	x		x		(x)	x		x	x			dd
M0801382		x		x	x				x		x			?	gr
M1002603	x			x			x		(x)		x			x	gr
		x		x			x		x		x	x			dd
M0800498		(x)		x	x				x	?				x	gr
M0904682		x		x			x		x		x			x	gr
M0705326		x		x	x				x		x			x	gr
M0100798		x		x	x				x		x			x	gr
M0901492		x		x	x				x	?				x	gr

[a]Because of space limitations, only the images discussed in the text from the mission phases September 1997 to August 1999, and September 1999 to February 2000 are listed. The classification is the base for the distribution map in Figure 6a. Abbreviations as follows: dd, dust devil track; gr,groove; fr,fracture; fluv, fluvial. An empty space in the MOC image number column represents a second prominent occurrence of LCF in the image with the number listed just above. Parentheses indicate less apparent and question marks indicate uncertain.

without making any deep impression on the surface. However, other LCFs appear either to have a subsurface continuation, or to form shallow grooves or ridges on the surface. On the basis of the classification in Table 1, we have sorted the LCFs into three main groups:

[12] 1. Group 1 consists of straight or curved streaks apparently affecting only the surface. These streaks may be solitary or densely distributed. Examples of this group are shown in Figure 1.

[13] 2. Group 2 consists of straight or curved lines that appear to have a subsurface extension. Some in this group are surprisingly independent of the surface topography and can continue straight across the rim of a crater, whereas others bend or change direction. Polygonal patterns also occur. Examples of this group are shown in Figure 2.

[14] 3. Group 2 consists of single or densely distributed lines that form grooves in the surface. Some show prominent elevated rims. Examples of this group are shown in Figures 3–5.

[15] The mapping displayed in Figure 6a and the comparison with the MOLA topography in Figure 6b show that group 1 is most common and occurs all over the Hellas basin, group 2 occurs only in a few locations, mainly in the periphery of the basin, and group 3 occurs sporadically in the deeper, northern and western parts of the basin as well as along its rim. Many of the densest occurrences of LCFs in the Hellas have general SW-NE to NW-SE directions, but E-W directions also occur. The temporal variation of LCFs of group 1 is exemplified in Figure 7. Figure 7 shows two sections of the images M1100046 and M1401193. The time interval between the images is $\sim$3.5 months. The sections labeled A and B show LCFs that apparently have changed only slightly during this time, whereas a complete change is visible in the sections C and D. The observed temporal changes indicate an active process that affects the surface, most likely dust devils.

[16] The results from the study of the influence of resolution and incidence angle are shown in Figure 8. There is a strong difference in detection of LCFs between the early phases (September 1997 to August 1999) and later phases (September 1999 to February 2000) of MOC images. The later phases have a much higher proportion of images containing visible LCFs than the earlier phases.

4. Discussion

4.1. Factors Affecting the Detection

[17] From the graphs, there appears to be a slight increase of average resolution from the early phases to the later phases. The high percentage of high-resolution images (1–3 m) among the empty images of both the early and the later phases show that differences in image resolution on the scale 1–12 m (i.e., standard MOC image) have only a minor influence on the detection of LCFs. However, there is a higher proportion of low-resolution images in the early empty images than in the later empty images. There is also a slight difference in image resolution distribution between empty and good images. Thirty-five percent of the empty images of the early phases (September 1997 to August 1999) have an image resolution of 11–12 m, whereas the resolution apparently is a little higher for the good images. The same slight difference exists between empty and good images of the later phases (September 1999 to February 2000). This difference would be expected if resolution plays a role. Images with incident angles of a medium range (25°–50°) increased in the later phases, whereas images

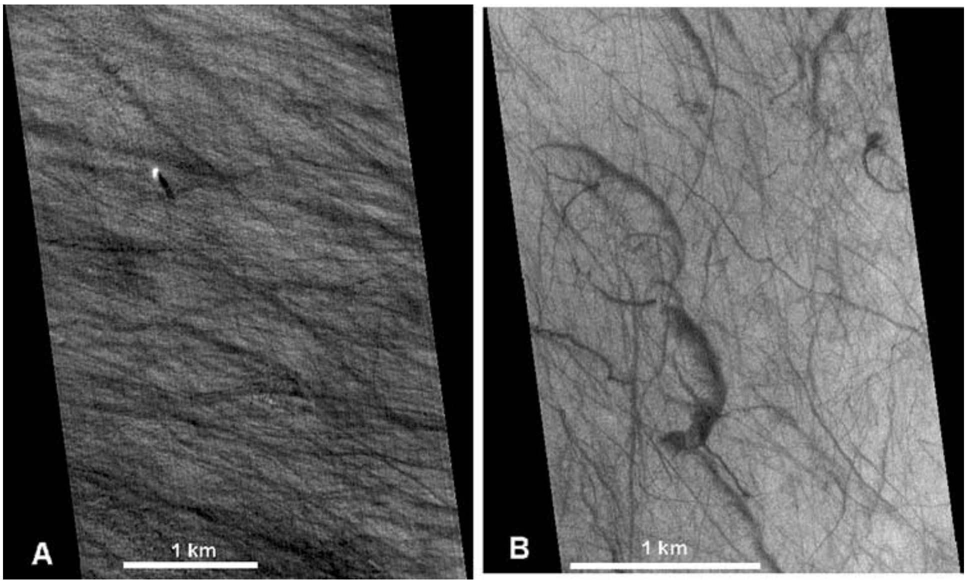

Figure 1. Examples of LCFs of group 1. In this group the streaks appear to affect only the ground surface. They are most likely dust devil tracks. (a) Section of M1201292. The surface is densely striated by mainly straight linear features. The white dot is most likely an active dust devil. (b) Section of M1002813. Surface with curved LCFs.

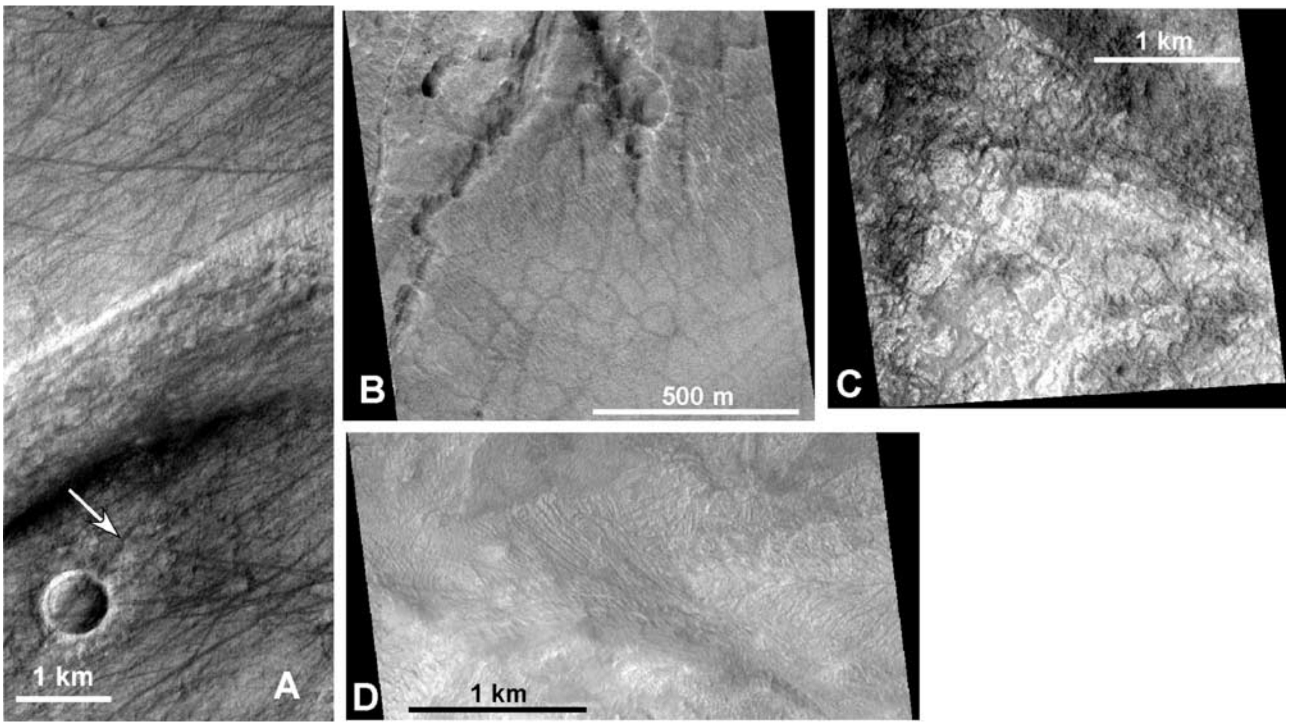

Figure 2. Examples of LCFs of group 2. The LCFs appear to have a subsurface extension. The LCFs in this group have a rather straight outline although they sometimes form a polygonal pattern. They appear independent of topography and sometimes penetrative (note the illuminated rim at the arrow in Figure 2a). We classify them as possible surface expressions of fractures. Some overprinting of dust devil tracks may occur, but it is doubtful that all lines are such tracks. (a) Section of M0701142. Note how one LCF is crossing the topography of the rather fresh impact crater. (b) Section of M1200407. Dark lines are forming a polygonal pattern. In the upper part of the image collapse expands the fractures. (c) Section of M1001828. Crisscrossing dark lines that appear to penetrate the surface. A polygonal pattern indicates a similar genesis as in Figure 2b. (d) Section of M0701980. LCFs are penetrating the surface. They are classified as fractures, but some rims of LCFs in the central part of the image appear to have elevated rims, which are more consistent with grooves.

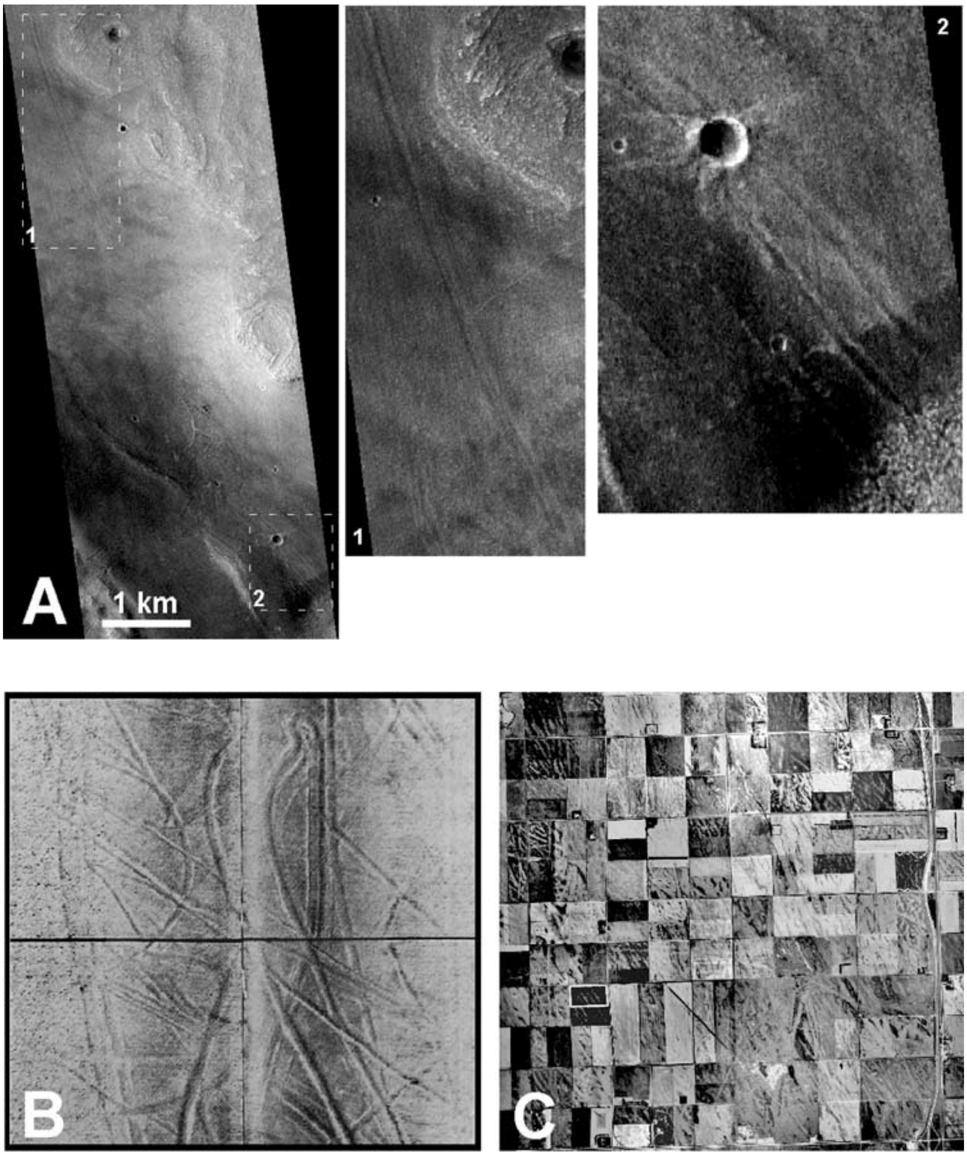

Figure 3. Examples of LCFs of group 3. This group includes the LCFs that appear to be grooves in the ground. (a) Section of M1002603 with magnifications of selected areas (boxes 1 and 2). Image resolution is 2.78 m pixel^{-1}. The image shows grooves on a smooth valley floor. A groove in the selected area 1 divides into two narrow, parallel grooves in the lower part of the selected area. Note how the crater in the selected area 2 is superimposed on two parallel grooves. (b) Sonar image of iceberg plow marks on the North American Atlantic shelf. The image is 600 $\times$ 600 m. The dimensions and appearance of the terrestrial plow marks are consistent with the Martian LCFs. A double keeled iceberg has generated parallel grooves at the image center. Image courtesy of Klein Associates Inc. (c) Section of the former glacial Lake Agassiz, North Dakota. The image is 9 $\times$ 9 km. The square pattern is due to farmland. Of interest is the pattern of streaks that is faintly visible in the background. The streaks are from iceberg plow marks that are still visible as shallow grooves despite extensive cultivation and other erosional and depositional processes. This shows that ancient plow marks in the Hellas basin could still be visible even after being subject to wind erosion. Image courtesy J. Bluemle, North Dakota Geological Survey.

with incidence angles of a high range (50°–80°) decreased in the later phases. It can also be seen how the empty images in the later phases are skewed toward higher angles, whereas the good images are skewed toward lower angles. This is what could be expected if the majority of the LCFs are due to differences in surface albedo (i.e., dust devil tracks). It can be concluded that in the later phases, detection of LCFs increased, most likely because of a combination of higher image resolution and an increased number of medium-range incidence angle images. Likewise, images with no visible LCFs decreased, possibly because of the lack of high incidence angle images and higher resolution. These observations indicate that the increased detection of LCFs in the later phase appears to be at least partially due to the incidence angle change, possibly in combination with a generally slightly higher

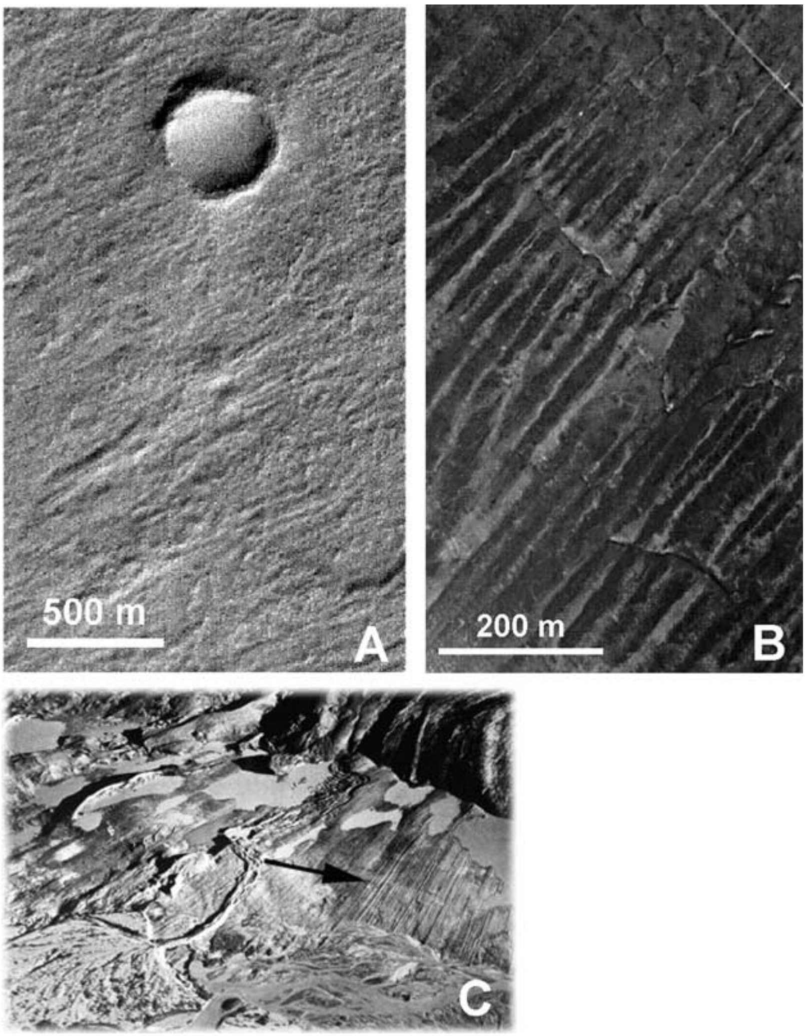

Figure 4. Example of LCFs of group 3. (a) Section of image M0202679. Grooves are indicated with illuminated rims or narrow parallel ridges. Trenches with elevated rims are known from iceberg plow marks on oceanic shelves on Earth. Other similar terrestrial features are fluted moraines. Yardangs are also possible, but they do not usually have a central trench traceable for a long distance. (b) Fluted moraines on the Pas Moraine, Canada. Their relief is only a few meters high. Landsat Near-Infrared image. From http://daac.gsfc.nasa.gov/DAAC_DOCS/geomorphology/GEO_9/GEO_PLATE_G-21.HTML. (c) Fluted moraines at the front of a terrestrial glacier. Note the parallel grooves and ridges at the arrow. Photograph by B. Washburn. From http://www.glacier.rice.edu/land/5_depositionalsubglacial.html.

image resolution. Of course, we cannot rule out that some event may have generated many new LCFs after the early phases. If the majority of the newly detected LCFs are dust devil tracks, this would imply an increase in dust devil activity in the Hellas basin in the later phases.

4.2. Possible Processes of Formation

4.2.1. Dust Devils

[18] Wind is the only surface-shaping factor that is known to presently be active over a short geological timescale on Mars. The dust devil observed in Figure 1 among the dark LCFs of group 1, the apparent relation between most LCFs and the incidence angle, and the clear temporal variation of LCFs of group 1 in Figure 7 support that dust devil action can be considered the most likely cause for the LCFs of group 1. This group is, by far, the most common in the Hellas basin (Figure 6a). The frequent occurrence of dust devil tracks in the interior of the Hellas Planitia may be influenced by the thicker atmosphere in this deep basin. In Figure 6, the general trend of directions of dust devil tracks appears to be SW-NE to NW-SE. This suggests that a preferred wind direction is responsible for the movement of the dust devil vortices over the surface. The atmospheric Global Circulation Model (GCM) of Mars indicates somewhat complex N-S and E-W wind patterns [*Greeley et al.*, 1992]. This differs somewhat from the main directions of the dust devil tracks we have mapped. However, *Greeley et al.* [1992] used Viking-based topography for their GCM. More studies on the link between dust devil tracks and general wind direction using MOLA data may be needed before it can be concluded that the local wind patterns in the Hellas basin are different from the results derived from the

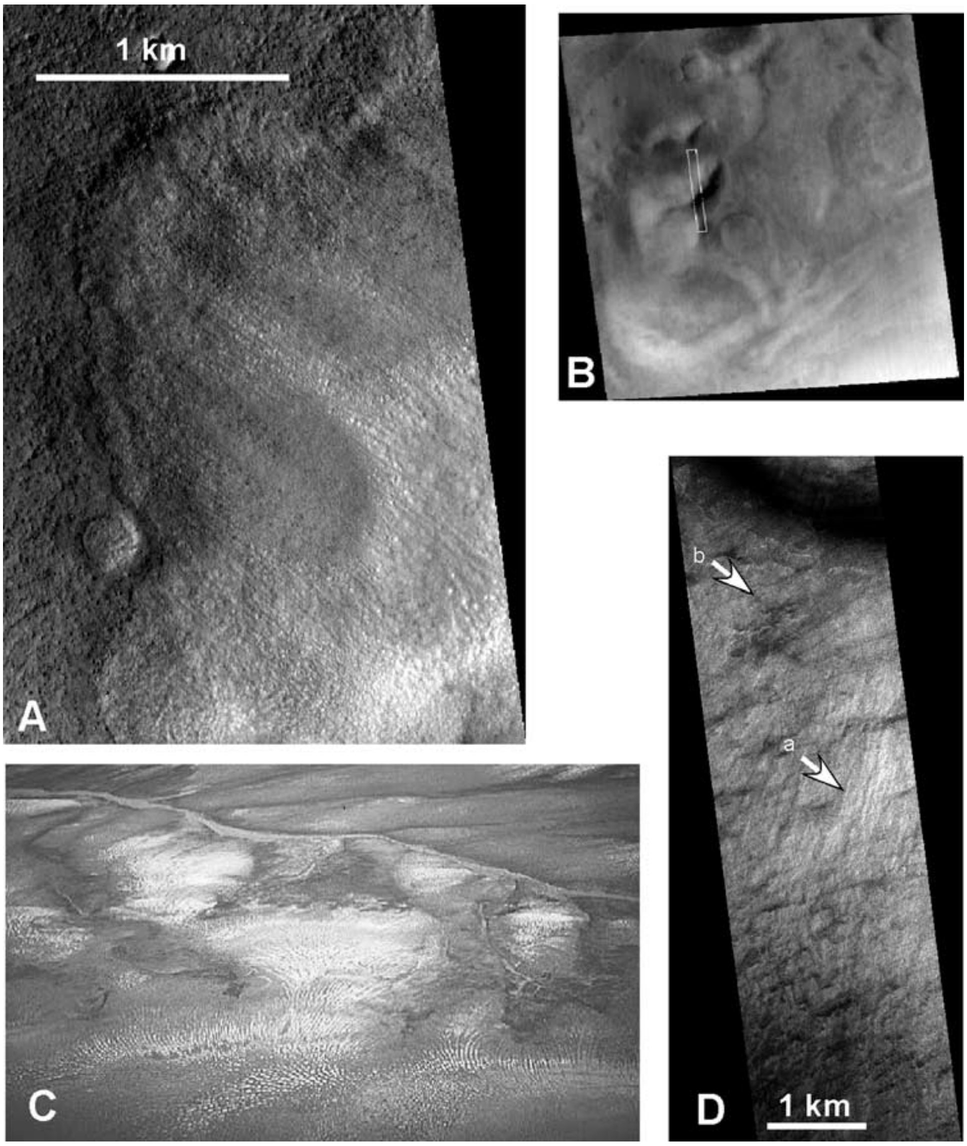

Figure 5. Examples of LCFs of group 3. Section of (a) M0705326 and (b) M0705327 context image. The section in Figure 5a covers only a part of the shadowed slope in Figure 5b. The LCFs closely resemble terrestrial cryoturbation patterns. Alternatively, they could be striated ejecta. However, the only crater in the vicinity is eroded and has no visible ejecta. The striations are also slightly bent, which make the ejecta alternative less likely (compare with the striated ejecta in Figure 5d). (c) Cryoturbation patterns, Canada. The lines are small ridges of soil. The image is ~1 km wide. From Natural Resources Canada (http://sts.gsc.nrcan.gc.ca/clf/landscapes.asp). (d) Striated ejecta (arrow a) from crater in upper part of the image. Section of M1002592. The lines are straight and parallel. The other, dark lines (arrow b) are considered dust devil tracks.

Greeley et al. [1992] GCM simulation. In addition to a denser atmosphere, it is possible that the many LCFs observed in the deeper parts of the Hellas may be the result of a more extensive dust cover of these areas (easier to generate dust devil tracks) and the fact that these areas are relatively flat (easier to observe dust devil tracks) compared to the rim and surroundings. *Tanaka and Leonard* [1995] had already suggested a dominantly fine-grained infill of the Hellas basin before the reception of MOC images.

[19] Most of the LCF we have classified into the first group are similar to the dust devil tracks presented by *Malin and Edgett* [2001]. However, the great variety in appearance of the LCFs of the other two groups makes it unlikely that they are the result of just one process. The LCFs of these groups differ significantly from the appearance of known dust devil tracks, although there may be some transitional morphologies and also overlapping cases (e.g., Figures 2 and 5).

4.2.2. Periglacial and Fluvial Features

[20] A striation apparently caused by fluvial activity is noted in image M0903721. The interpretation is based on the appearance of the striations parallel to the channel of Harmakhis Vallis. It is the only one in the MOC images examined in this study, although more examples of fluvial striation are likely to be found in the future with a denser coverage of

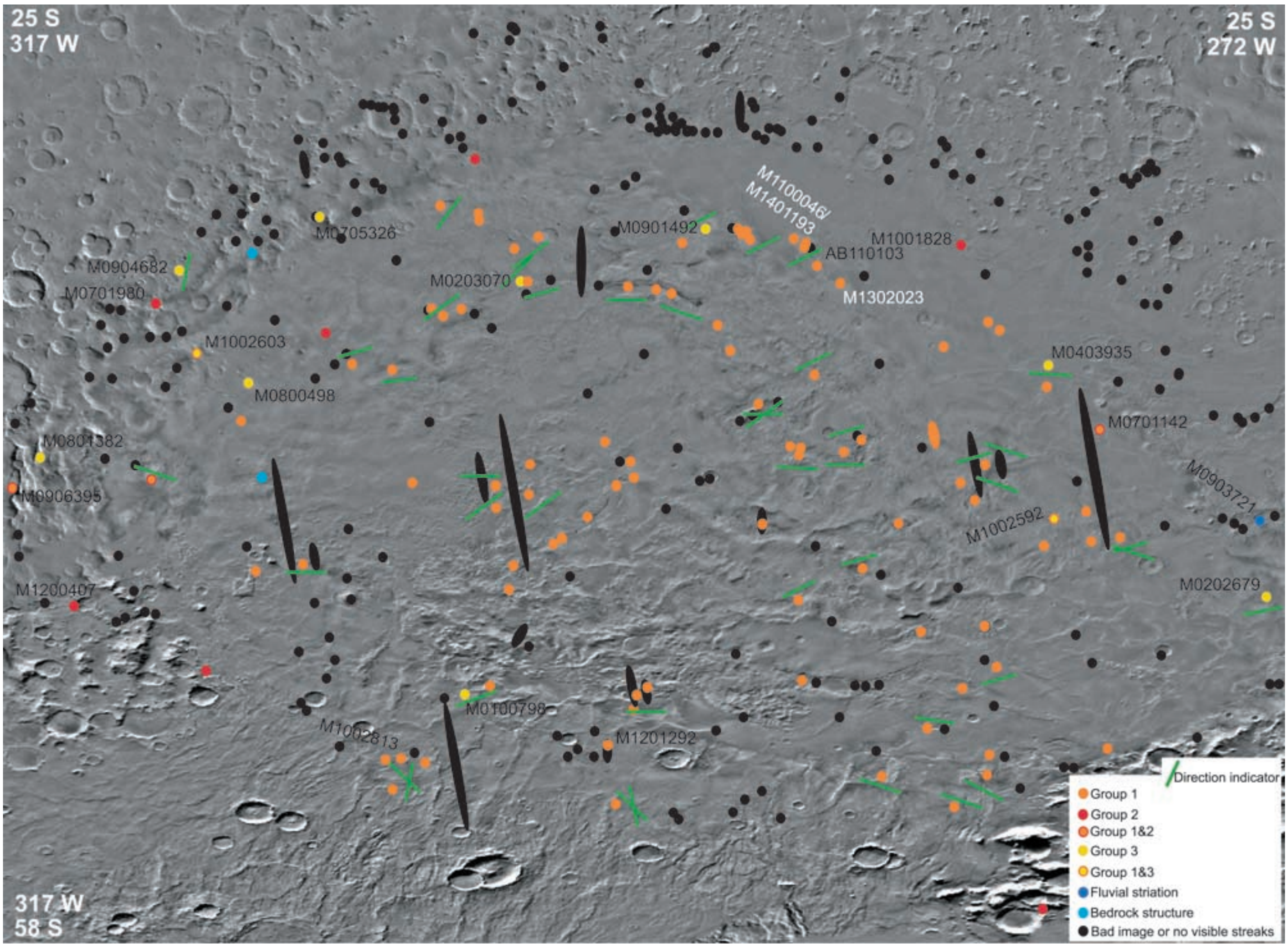

Figure 6a. Map showing locations of all images used in this study. The color coding represents the groups into which we have interpreted the LCFs visible in each image. The dominant direction(s) of the LCFs in each image is indicated with a green line. Images discussed in the text and listed in Table 1 are indicated by their numbers. White image number indicates that the image is from a more recent phase than the other images used (September 1997 to February 2000).

MOC images. More interesting are the LCFs classified as group 2 in Figure 2. In general, they form polygonal patterns that can be clearly seen in the surface topography. Their morphology suggests that they are fractures, possibly comparable to terrestrial ice wedges. Similar features elsewhere on Mars have been proposed to be large-scale analogues to terrestrial tundra polygons [*McGill*, 1986]. MOC images reveal many small-scale, contraction crack polygons that even more closely resemble these terrestrial counterparts [*Seibert and Kargel*, 2001]. Subsurface ice may be indicated by the collapse expansion of the fractures in Figure 2b. The LCFs in Figure 2a are different. They have an appearance that is similar to dust devil tracks (Figure 1). However, some appear to have parts that penetrate the surface to form either a groove or a trench. A dominant LCF crosses straight over an almost 1 km wide, fresh crater. Following the standard crater morphology [*Melosh*, 1989], and with respect to the lower gravity of Mars, such a crater would have an elevated rim $\sim$50–70 m high, with a rather steep rim wall, and be more than 200 m deep. It seems unlikely that a dust devil would pass this topographic feature without changing direction. Fractures could, however, cross the crater in this way if they postdated the crater. Preexisting fractures would be overprinted by the impact fracturing and not visible over the breccia lens of the crater interior.

[21] An example of very tightly spaced ridges and grooves of the sort found in group 3 occurs on a hillside in the northwestern periphery of the Hellas basin (Figures 5a and 5b). The striations closely resemble terrestrial cryoturbation patterns (Figure 5c). An alternative could be striated ejecta, like the grooves and ridges in Figure 5d. However, the only possible source in the vicinity is an eroded crater with no other visible ejecta. The striations are also slightly bent, which makes the ejecta alternative less likely. Cryoturbation patterns represent a periglacial landform that forms when freeze-thaw heaves soil to the surface. Creep stretches the patches into long stripes.

[22] Periglacial landform formation requires an environment more different from present-day Mars than the glacial formation does [*Baker*, 2001]. This is particularly true for the temperature regime. That the identified periglacial morphologies in the Hellas basin appear young, testifies a significant shift in Martian climate in recent past.

4.2.3. Glacial Features

[23] Some of the LCFs in the third group are interesting because their grooved morphology could indicate a process

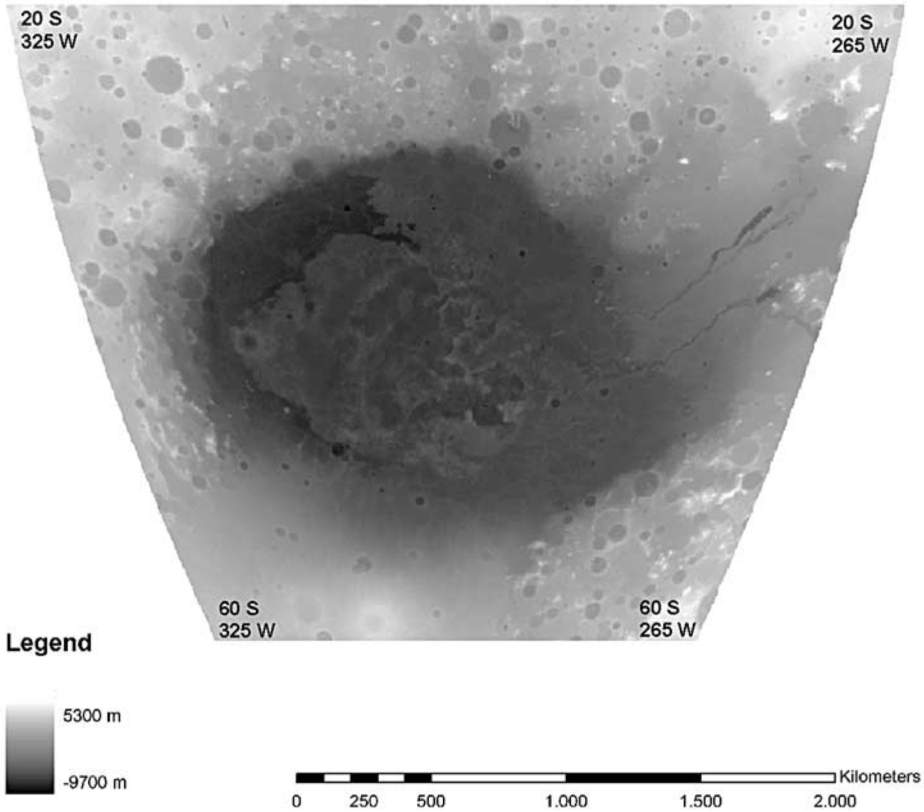

Figure 6b. MOLA base map of the Hellas basin.

capable of scouring the surface. On Earth, such scouring is most often related to moving land ice. *Komatsu et al.* [2000] argued that some of the LCFs could be iceberg plow marks formed in a proglacial lake. Iceberg plow marks form when an iceberg drifts into areas with water depths less than the iceberg's keel depth. On Earth the troughs that form in the seafloor are ~0.5–5 m (rarely 25 m) deep. They may be flanked by berms up to 2 m high [*Lien*, 1983; *Vogt et al.*, 1994]. In the study by *Vogt et al.* [1994] of the North Atlantic Yermak Plateau, the plow marks are usually a couple of hundred meters to some kilometers long but some can continue for tens of kilometers and be tens to hundreds of meters wide. These figures are consistent with the sizes of the LCF seen in our study area. In connection with terrestrial plow marks, 30–150 m wide, semicircular, flat-floored depressions may occur. These "iceberg craters" form when icebergs run aground in shallow water. In places where the water is so shallow that an iceberg runs aground before it can cross, the iceberg suspends sediments that form a shoal inboard of a sharp knickpoint [*O'Brien et al.*, 1997].

[24] *Komatsu et al.* [2000] used the image AB110103 in their argumentation. In addition to plow marks they suggested that some other features were also iceberg craters. However, after comparison with similar LCFs visible in adjacent images (e.g., Figure 7 and image M1302023), we believe that these LCFs are dust devil tracks. This reinterpretation is also supported by the fact that the general direction of the LCFs in the image is the same as more obvious dust devil tracks in adjacent images. Nevertheless, overprinting of dust devil tracks on a surface with shallow grooves can not be excluded given the few images available at present. More evident groove-like LCFs appear in Figure 3. They occur as single (Figure 3a, area 1) or as a few parallel grooves (Figure 3a, area 2). The setting is a flat valley floor near the western rim of Hellas. Some of the parallel grooves are cut by a more recent impact crater. In area 1 in Figure 3a the groove changes in shape and divides into two shallow, attached grooves. The illuminated elevated rims are clearly visible. The grooves show a striking resemblance to iceberg plow marks on the North American Atlantic shelf (Figure 3b) and in the former glacial Lake Agassiz, North Dakota (Figure 3c). A change in shape, like the split seen in area 1 in Figure 3a, is common among plow marks and is due to rotation of the iceberg and abrasion of its keel. The elevated rims in areas 1 and 2 in Figure 3a may represent berms like those associated with plow marks on Earth.

[25] Of course, we cannot rule out the possibility that these grooves were formed by some other processes. However, we believe dust devils can be discarded due to the apparent depths of these grooves. *Metzger* [2001] estimate the average vertical flux of dust in the Martian dust devils to be 0.5 g m^{-2} s^{-1}. Hence it appears unlikely that a dust devil can generate grooves of the dimensions in Figure 3 even if the substrate is entirely made up of dust.

[26] The distribution of LCFs of group 3 in the Hellas basin to some extent coincides with the location of the proglacial lake proposed by *Kargel and Strom* [1992] and the ice covered lakes suggested by *Moore and Wilhelms* [2001]. It can be argued that if a proglacial lake existed in

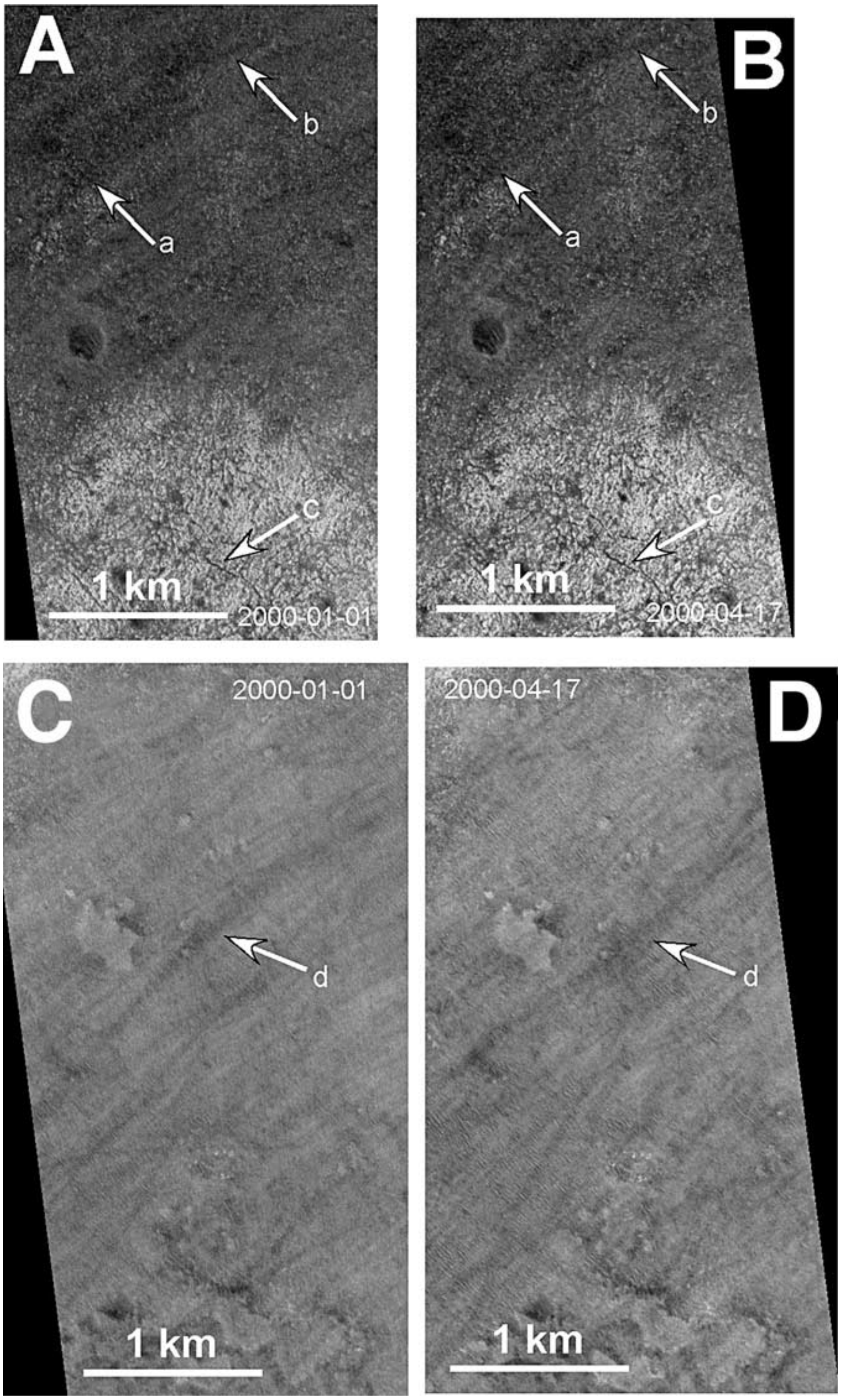

Figure 7. Comparison of two images from the same area obtained with a few months interval. (a and c) Two sections of image M1100046 obtained in January 2000. (b and d) Two sections of image M1401193 obtained in April 2000. Dark LCFs at arrows a and b show that some LCFs remain at least some months, whereas other LCFs can disappear completely and new are formed (location indicated by arrow d). Our interpretation is that these LCFs are dust devil tracks. Location indicated by arrow c shows LCFs of a different character. They are penetrative and remain unchanged between the two occasions. They are probably fractures. The incidence angle is about the same for both images (25.47° and 29.75°).

the Hellas basin, an iceberg-producing, calving front must have existed as well. At most locations on Earth where icebergs are produced, scouring of the seafloor also occurs. *Moore and Wilhelms* [2001] reject the hypothesis of continental glaciation by *Kargel and Strom* [1992]. Instead, they suggest a model where outflows of water through the channels in the east and south of the basin produced large standing bodies of water in the deeper parts of Hellas. These

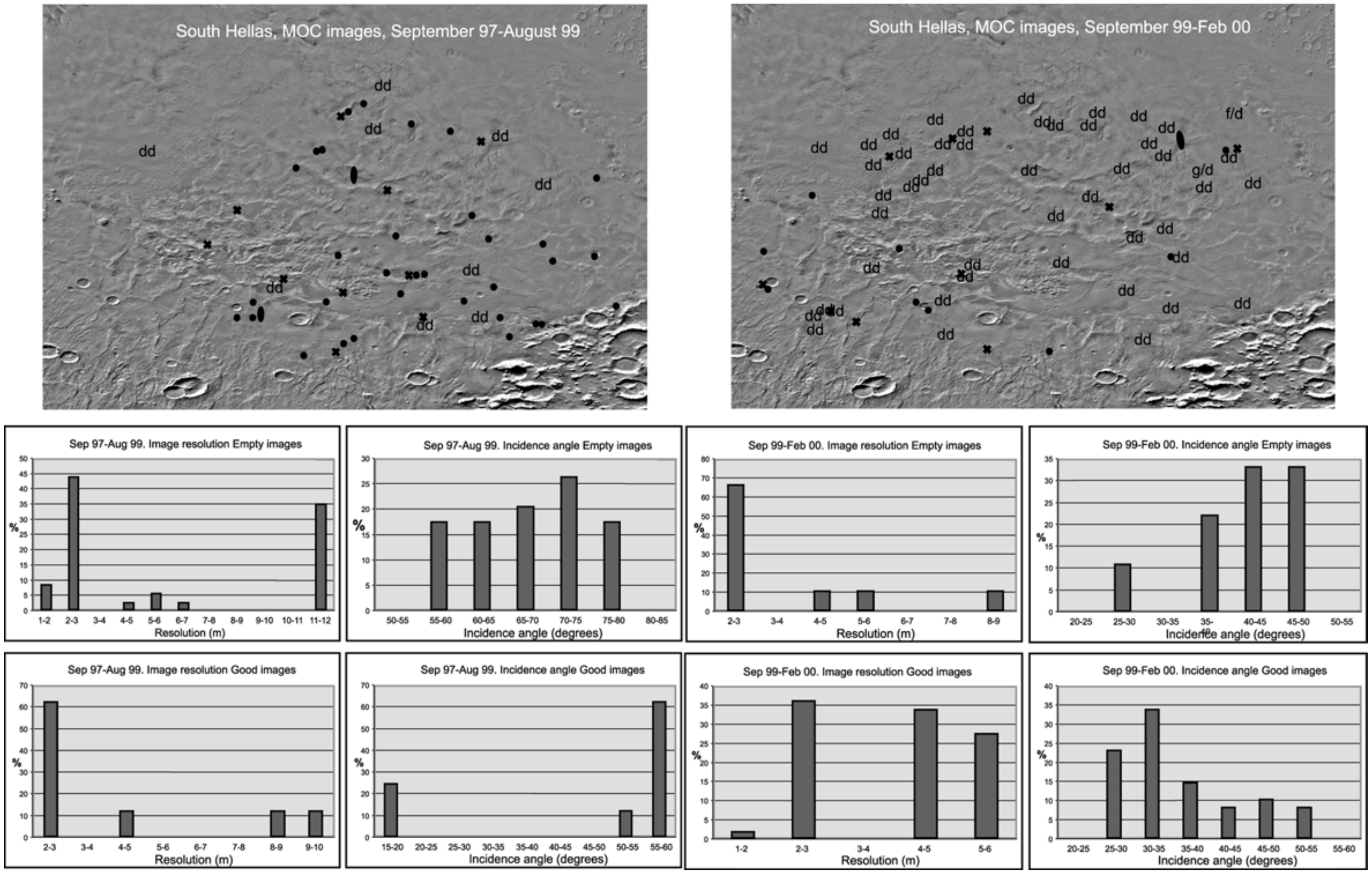

Figure 8. Plots showing occurrence of LCFs on the surface of Mars classified according to image resolution and incidence angle. Images with LCFs are marked with abbreviations of their classification (dd dust devil tracks, g/d grooves and dust devil tracks, f/d fractures with dust devil tracks). These images are labeled good in the plots. Black dots are images with no visible LCFs (labeled empty in the graphs). Black crosses are corrupted images (not included in the graphs). There is a strong difference in detection between early and later phases of MOC images. There appears to be some influence by the image resolution. However, the correlation with the incidence angle may be more significant. A lower angle seems to favor detection. This is what can be expected for features caused by differences in surface albedo (e.g., dust devil tracks).

water bodies are thought to have developed ice carapaces several hectometers thick. In some areas in the western part of the basin (near the locations of the images M1002603 and M0800498) it is suggested that the carapaces became grounded. We do not know if such thick ice carapaces can produce features similar to iceberg plow marks. However, this appears likely if there are forces available that can cause horizontal movements of partially grounded sea ice (e.g., tidal forces). The grooves in Figure 3 are confined to a valley coming out from the rim area of the Hellas. This valley may have hosted a glacier flowing into a transient lake. The valley ends in the deepest part of the basin (Figures 6a and 6b) and water could have existed there without ice sheet type glaciation. Nevertheless, the presence of glaciers at the inner rim area requires precipitation, at least regionally, and the Hellas may have hosted many Alpine type glaciers ending in lakes of perhaps considerable size. Hence our observations of possible iceberg plow marks neither confirm nor contradict the continental style glaciation proposed by *Kargel and Strom* [1992].

[27] The example of Lake Agassiz shows that iceberg plow marks can be visible even after years of relatively strong surface erosion by farming and cultivation of the land (Figure 3c). Hence a proglacial lake in the Hellas basin should have left visible plow mark features. We believe that such features, although rare, are visible in some areas of the Hellas. The spatial coverage of high-resolution MOC images on the Mars surface is still very limited. Since identification of such grooves requires high-resolution images and also good photographic geometries, it is possible that future MOC images will reveal more examples of LCFs that can be interpreted as iceberg plow marks.

[28] Figure 4a shows an additional type of groove-like LCF. These LCFs are rather tightly spaced, of equal width and very straight. The most similar terrestrial analogue is fluted (ground) moraine. Fluted moraine forms in soft, water saturated material behind obstacles under the front of a moving glacier. As the glacier recedes, these lineations or streamline features may be visible in older drift or freshly deposited till in front of the moving ice. [*Sugden and John*, 1976]. Fluted moraine is a positive feature. However, where the ridges are tightly spaced, it may look like groove-like depressions between them. Examples of terrestrial fluted moraines are shown in Figures 4b and 4c. In addition to the image in Figure 4a, possible fluted moraine is also visible in image M0100798. These images are all located at the periphery of the Hellas basin in areas that once may have been affected by the receding ice, as proposed in the Kargel and Strom hypothesis.

[29] If our interpretation of some LCFs as plow marks is correct, their formation could be explained by either models proposed by *Kargel and Strom* [1992] and *Moore and Wilhelms* [2001]. However, the presence of possible fluted moraine supports the widespread glaciation in the Hellas basin suggested by *Kargel and Strom* [1992]. The importance of ancient glaciers on Mars is that they would have required snow precipitation and, hence, sources of water. The proposed northern plain ocean [*Parker et al.*, 1989; *Baker et al.*, 1991; *Head et al.*, 1999] may have provided the water. The question remains if any of the proposed oceanic phases existed long enough for land ice to evolve. If, as suggested above, icebergs played roles in the formation of some landforms, they provide information on the deglaciation processes. A deglaciation involving the formation of icebergs and fluted moraine imply that the supply of snow was eventually shut off, but that the ice receded in a relatively warm environment. It is evident that other processes have been active in the Hellas basin in addition to eolian. The existence of glacial and periglacial features in Hellas has important paleoclimatic implications. Therefore it is important to examine these and related features in more detail by further MOC image analysis and other methods.

5. Conclusions

[30] Our study of linear and curvilinear features (LCFs) on Mars, with special focus on the Hellas basin, the following were found

[31] 1. The LCFs are frequent in the Hellas basin, and sometimes occur densely.

[32] 2. The majority of the LCFs in the central parts of Hellas are consistent with known dust devil tracks.

[33] 3. Some LCFs appear to penetrate the surface and are more consistent with fractures. They are most likely periglacial landforms such as ice wedge fractures.

[34] 4. Some LCFs appear to be grooves and depressions between narrow, parallel ridges. They are most likely glacial and periglacial landforms such as iceberg plow marks, fluted moraines, and cryoturbation patterns.

[35] The high concentration of dust devil tracks in the Hellas indicates ideal conditions for dust devil formation in this area, possibly due to the denser atmosphere in combination with abundant dust on wide, smooth areas in this low-lying location. The existence of possible glacial and periglacial landforms supports earlier suggestions about ancient glaciations in the Hellas region. The type of landforms observed indicates that the ice receded in a warm climate.

[36] **Acknowledgments.** The authors acknowledge the use of Mars Orbiter Camera images processed by Malin Space Science Systems that are available at http://www.msss.com/moc_gallery/. We thank Stefano Di Lorenzo and Paolo Sammartino of IRSPS for producing the Hellas MOLA base map, anonymous reviewers for valuable comments, and Carol Cleland for help with the linguistics.

References

Albin, E. F., and J. D. King, Dark slope streaks and associated layered deposits on the southwestern floor of Cassini impact basin, Mars (abstract), *Lunar Planet. Sci.* [CD-ROM], *XXXII*, 1380, 2001.

Baker, V. R., Water and the Martian landscape, *Nature*, *412*, 228–236, 2001.

Baker, V. R., R. G. Strom, V. C. Gulick, J. S. Kargel, G. Komatsu, and V. S. Kale, Ancient oceans and ice sheets and the hydrological cycle on Mars, *Nature*, *352*, 589–594, 1991.

Balme, M., R. Greeley, B. Mickelson, J. Iversen, G. Beardmore, D. Branson, and S. Metzger, Dust devils on Mars: Results from Threshold tests using a vortex generator (abstract), *Lunar Planet. Sci.* [CD-ROM], *XXXIII*, 1048, 2002.

Edgett, K. S., M. C. Malin, R. J. Sullivan, P. Thomas, and J. Veverka, Dynamic Mars: New dark slope streaks observed on annual and decadal time scales (abstract), *Lunar Planet. Sci.* [CD-ROM], *XXXI*, 1058, 2000.

Grant, J. A., and P. H. Schultz, Possible tornado-like tracks on Mars, *Science*, *237*, 883–885, 1987.

Greeley, R., N. Lancaster, S. Lee, and P. Thomas, Martian eolian processes, sediments and features, in *Mars*, edited by H. H. Kieffer et al., pp. 730–766, Univ. of Ariz. Press, Tucson, 1992.

Greeley, R., J. D. Iversen, G. Beardmore, B. Mickelson, and S. Metzger, Martian dust devils: Laboratory simulations (abstract), *Lunar Planet. Sci.* [CD-ROM], *XXXII*, 1888, 2001.

Head, J. W., III, H. Hiesinger, M. A. Ivanov, M. A. Kreslavsky, S. Pratt, and B. J. Thomson, Possible oceans on Mars: Evidence from Mars Orbiter Laser Altimeter data, *Science*, *286*, 2134–2137, 1999.

Kargel, J. S., and R. G. Strom, Ancient glaciation on Mars, *Geology*, *20*, 3–7, 1992.

Komatsu, G., A. P. Rossi, and J. S. Kargel, Glacier landforms identified in MOC images, Mars (abstract), *Bull. Am. Astron. Soc.*, *31*(4), 1133, 1999.

Komatsu, G., A. P. Rossi, J. Ormö, and J. S. Kargel, Glacier landforms in the northeastern Hellas basin (abstract), *Lunar Planet. Sci.* [CD-ROM], *XXXI*, 1451, 2000.

Lien, R., Iceberg scouring on the Norwegian continental shelf, *Offshore Technol. Conf. Proc.*, *3*, 41–48, 1983.

Malin, M. C., and K. S. Edgett, Mars Global Surveyor Mars Orbiter Camera: Interplanetary cruise through primary mission, *J. Geophys. Res.*, *106*, 23,429–23,570, 2001.

McGill, G. E., The giant polygons of Utopia, northern Martian plains, *Geophys. Res. Lett.*, *13*, 705–708, 1986.

Melosh, H. J., *Impact Cratering: A Geologic Process*, 245 pp., Oxford Univ. Press, New York, 1989.

Metzger, S. M., Recent advances in understanding dust devil processes and sediment flux on Earth and Mars (abstract), *Lunar Planet. Sci.* [CD-ROM], *XXXII*, 2157, 2001.

Metzger, S. M., J. R. Johnson, J. R. Carr, T. J. Parker, and M. Lemmon, Dust devil vortices seen by the Mars Pathfinder Camera, *Geophys. Res. Lett.*, *26*, 2781–2784, 1999.

Moore, J. M., and D. E. Wilhelms, Hellas as a possible site of ancient ice-covered lakes (abstract), *Lunar Planet. Sci.* [CD-ROM], *XXXII*, 1446, 2001.

O'Brien, P. E., G. Leitchenkov, and P. T. Harris, Iceberg plough marks, subglacial bedforms and grounding zone moraines in Prydz Bay Antarctica, in *Glaciated Continental Margins*, edited by T. A. Davies et al., 228–229, Chapman and Hall, New York, 1997.

Ormö, J., G. Komatsu, A. P. Rossi, and S. Di Simone, Thin Linear features on Mars visible in MOC images: The occurrences in the Hellas basin (abstract), *Lunar Planet. Sci.* [CD-ROM], *XXXII*, 1517, 2001.

Parker, T. J., R. S. Saunders, and D. M. Schneeberger, Transitional morphology in west Deuteronilus Mensae, Mars: Implications for modifications of the lowland/upland boundary, *Icarus*, *82*, 111–145, 1989.

Rossi, A. P., Possible dust devils tracks detected in Tenere' Desert (Niger): An analogue to Mars (abstract), *Lunar Planet. Sci.* [CD-ROM], *XXXIII*, 1307, 2002.

Seibert, N. M., and J. S. Kargel, Small-scale Martian polygons: Liquid surface water, *Geophys. Res. Lett.*, *28*, 899–902, 2001.

Sugden, D. E., and B. S. John, *Glaciers and Landscape: A Geomorphological Approach*, 376 pp., Arnold, London, 1976.

Tanaka, K. L., and J. G. Leonard, Geology and landscape evolution of the Hellas region of Mars, *J. Geophys. Res.*, *100*(E3), 5407–5432, 1995.

Thomas, P. C., and P. J. Gierasch, Dust devils on Mars, *Science*, *230*, 175–177, 1985.

Veverka, J., Variable features on Mars VIII-Dark filamentary markings on Mars, *Icarus*, *27*, 495–502, 1976.

Vogt, P. R., K. Crane, and E. Sundvor, Deep Pleistocene iceberg plowmarks on the Yermak Plateau: Sidescan and 3. 5 kHz evidence for thick calving ice fronts and a possible marine ice sheet in the Arctic Ocean, *Geology*, *22*, 403–406, 1994.

G. Komatsu, International Research School of Planetary Sciences, Universita d'Annunzio, Viale Pindaro 42, I-65127 Pescara, Italy. (goro@irsps.unich.it)

J. Ormö, Centro de Astrobiología, Instituto Nacional de Técnica Aeroespacial, Ctra de Torrejón a Ajalvir, km 4, E-28850 Torrejón de Ardoz, Madrid, Spain. (ormo@inta.es)